# CHAPTER II
# LITERATURE REVIEW

## 2.1 Bacterial Cellulose

### 2.1.1 Introduction to Bacterial Cellulose

Cellulose has been used daily for centuries in applications for making textiles, paper, plastic and food additives. It can be considered the oldest .The most abundant natural polymer. Cellulose consists of un-branched polymers of linked glucose residues arranged in linear chains where every other glucose residue is rotated 180 degrees. The glucose molecules are joined by a $C_1$–$C_4$ glucosidic oxygen linkage. Cellulose is a natural polymer of cellubiose. Celluboise is the structural repeating unit of the glucose chains in cellulose. Both adopt a stable $C_4$ chair conformation and hydrogen bonding between adjacent oxygen and hydrogen atoms forces a linear arrangement. Cellulose is a β-1, 4-glucan chain as shown in Figure 2.1

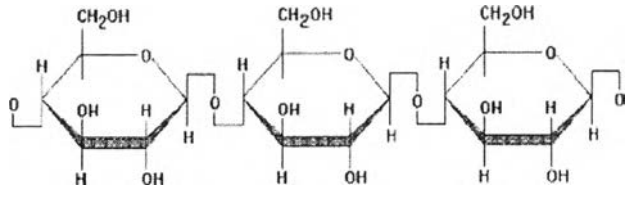


**Figure 2.1** Chemical structure of cellulose.

When the cellulose molecule is extended, it is a flat ribbon like structure that is further stiffened by Van der Waals forces and also by the hydroxyl groups protruding laterally which are able to form intra- and inter-molecule hydrogen bonds. The surface of the ribbon consists mainly of hydrogen atoms linked to carbon. The essential feature of cellulose is the primary and secondary alcohol groups in each monomer unit and the glucosidic unit bonds. The glucosidic bonds are not easily broken and therefore cellulose is very stable. The primary and secondary alcohol units in cellulose react in a similar manner as in simple substances of similar

chemical constitution. They may be readily oxidized, esterified and converted into ethers. The cohesive energy density of cellulose is high with the result that cellulose is insoluble in water. Although water vapor cm be absorbed strongly on fibrillar surfaces and in less ordered regions.

2.1.2 Principal Pathways to Cellulose

Up to now there are four different pathways to from the biopolymer cellulose as shown in Figure 2.2.

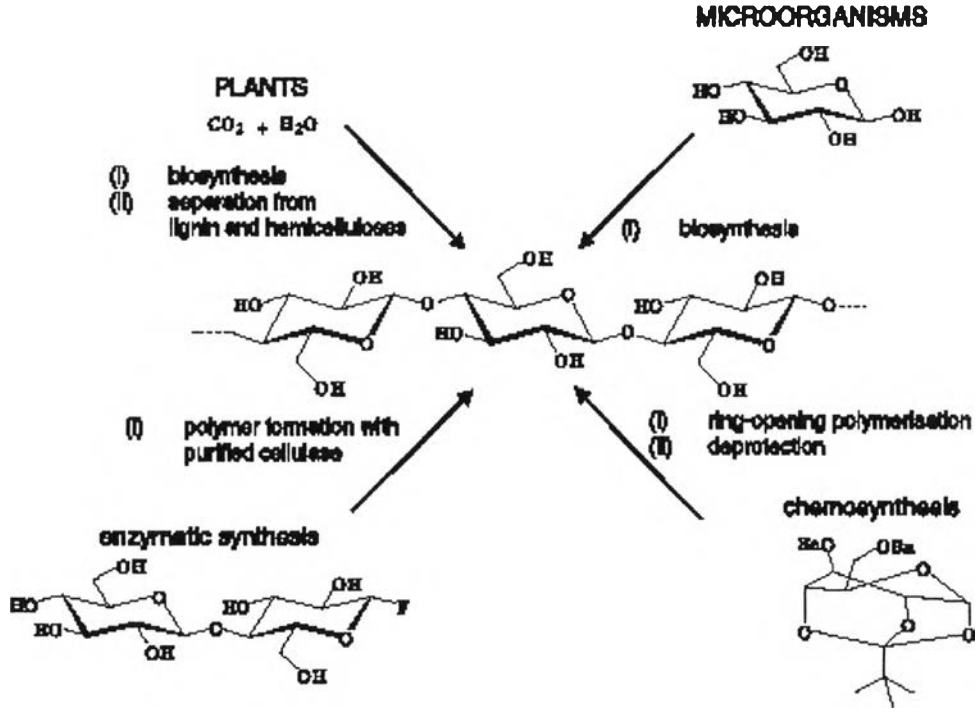


**Figure 2.2** Pathways for synthesizing of cellulose.

The first one is the most popular and industrial important isolation of cellulose from plants including separation processes to remove lignin and hemicelluloses (Tarchevsky & Marchenko, 1991). The second way consists in the biosynthesis of cellulose by different types of microorganisms. From the scientific point of view the first enzymatic in vitro synthesis starting from cellobiosyl fluoride and the first chemosynthesis from glucose by ring-opening polymerization of

benzylated and pivaloylated derivatives (Nakatsubo, Kamitakahara, & Hori, 1996) are of importance. These principle pathways are described schematically in Figure 2.2.

Several bacteria are in strains from the genera *Acetobacter, Agrobacterium, Pseudomonas, Rhizobium* etc. But not all these bacterial species are able to secrete the synthesized cellulose as fibers. Table 2.1 gives the overview. Special attention was given to strain from *Acetobacter xylinum* (Jonas & Farah, 1998).

**Table 2.1** Bacterial cellulose producers and feature of their product

| Genus | Cellulose structure |
|---|---|
| Acetobacter | Extracellular pellicle |
| Achromobacter | Fibrils |
| Aerobacter | Fibrils |
| Agrobacterium | Short fibrils |
| Alcaligenes | Fibrils |
| Pseudomonas | No distinct fibrils |
| Rhizobium | Short fibrils |
| Sarcina | Amorphous cellulose |
| Zoogloea | Not well defined |

2.1.3 Cellulose Synthesis Using *Acetobacter Xylinum*

*Acetobacter Xylinum*

*Acetobacter Xylinum* is a member of Family IV., Acetobacteraceae. This family is well known in the vinegar industry. The bacteria of this family convert ethanol to acetic acid. These are Gram-negative, rod-like shaped bacteria. They are strict aerobes. The optimum temperature range for growth is 25-30°C and the optimum pH range is *5-6. Acetobacter Xylinum* produces cellulose for two reasons; as a by-product of its metabolism and as an environmental defense mechanism. This

defense mechanism is used to allow the bacteria to float at the air-liquid interface so it can access oxygen and the media as well as protecting it from the harmful UV rays of the sun.

*Biosynthesis Pathway of Bacterial Cellulose*

According to the literature the cellulose formation includes five fundamental enzyme mediated steps; the transformation of glucose to UDP-glucose via glucose-6-phosphate and glucose-1-phosphate and finally the addition of UDP-glucose to the end of a growing polymer chain by cellulose synthase (Figure 2.3). Cellulose synthase (UDP-glucose: 1,4-β-d-glycosyltransferase) is regarded as the essential enzyme in the synthesis process. It is subjected to a complicated regulation mechanism, which controls activation and inactivation of the enzyme.

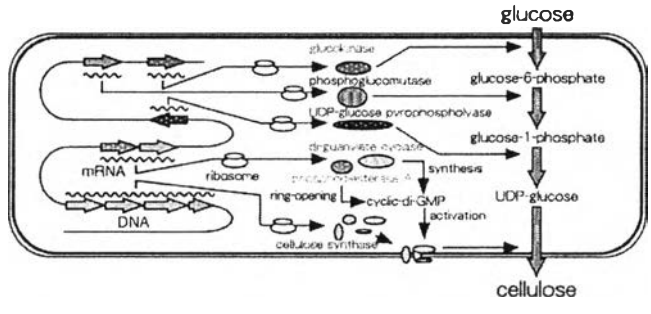


**Figure 2.3** Pathways of carbon metabolism in *Acetobacter Xylinum*.

*Acetobacter xylinum* forms the cellulose between the outer and the cytoplasma membrane. The cellulose-synthesizing complexes or terminal complexes (TC) are linearly arranged, and in association with pores at the surface of the bacterium. In the first step of cellulose formation glucan chain aggregates consisting of approximately 6 ±8 glucan chains are elongated from the complex. These subelementary fibrils are assembled in the second step to form microfibrils followed by their tight assembly to form a ribbon as the third step (Figure 2.4). The matrix of the interwoven ribbons constitutes the bacterial cellulose membrane or pellicle. Figure 2.5a shows bacterial cellulose ribbon produced by one bacterial cell and Figure 2.5b demonstrates that *Acetobacter xylinum* cells are distributed throughout the network of the cellulose ribbons (Tokoh, Takabe, Fujita, & Saiki, 1998).

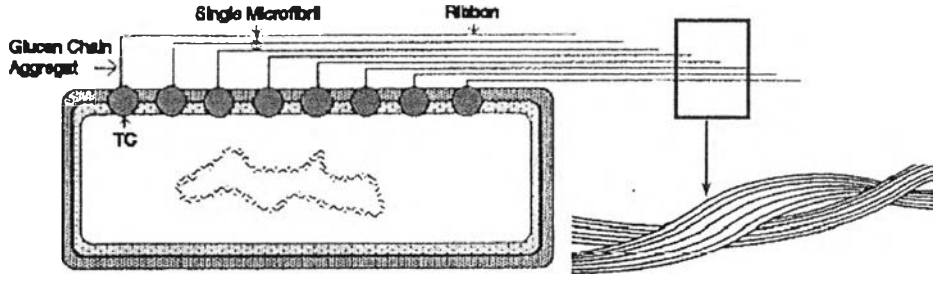


**Figure 2.4** Formation of bacterial cellulose ribbon.

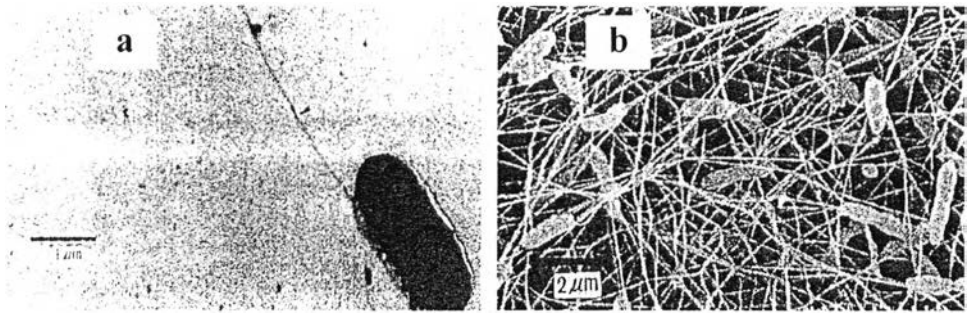


**Figure 2.5** SEM image of the bacterial cellulose ribbon produced by a bacterial cell (a) and the bacterial cellulose network including the bacterial cells (b).

*Structure Features and Properties of Bacterial Cellulose*

Bacterial cellulose revealed that it is chemically identical to plant cellulose, but its macromolecular structure differs from the latter. Bacterial cellulose microfibril is much smaller than that of plant cellulose. Bacterial cellulose is also distinguished from its plant counterpart by a high crystallinity index (above 60%) and different degree of polymerization, usually between 2000 and 6000 (Jonas, & Farah, 1998), but in some cases reaching even 16000 or 20000, whereas the average DP of plant polymer varies from 13000 to 14000. Macroscopic morphology of bacterial cellulose strictly depends on culture conditions (Watanabe, Tabuchi, Morinaga, & Yoshinaga, 1998; Yamanaka, Budhiono, & Iguchi, 2000). In static conditions, bacterial cellulose was produced in a form of leather-like pellicle on the surface of nutrient broth (Figure 2.6a). The subfibrils of cellulose are continuously

extruded from linearly ordered pores at the surface of the bacterial cell, crystallized into microfibrils, and forced deeper into the growth medium. Therefore, the leather-like pellicles supporting the population of Acetobacter xylinum cells consists of overlapping and inter twisted cellulose ribbons, forming parallel but disorganized planes (Jonas, & Farah, 1998). In agitated conditions, bacterial cellulose was produced in a form of irregular granules, well-dispersed in a culture broth (Figure 2.6b) (Vandamme, De Baets, Vanbaelen, Joris, & De Wulf, 1997).

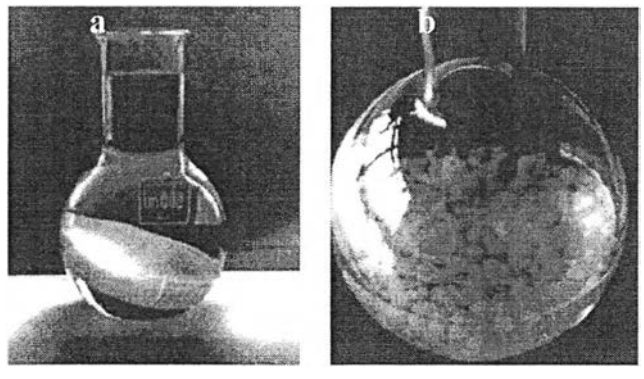


**Figure 2.6** Bacterial cellulose in the form of pellicle (a) and irregular granules (b).

## 2.2 Magnetic Particles

### 2.2.1 Introduction to Magnetic Nanoparticles

Magnetic nanoparticles are nanoparticles of iron oxide. Iron oxides exist in many forms in nature, with magnetite (Fe3O4), maghemite ($\gamma$-Fe2O3), and hematite ($\alpha$-Fe2O3) being probably the most common (Cornell & Schwertmann, 2003). Some of their physical and magnetic properties are summarized in Table 2.3.

Hematite is the oldest known of the iron oxides and is widespread in rocks and soils. It is also known as ferric oxide, iron sesquioxide, red ochre, specularite, specular iron ore, kidney ore, or martite. Hematite is blood-red in color if finely divided, and black or grey if coarsely crystalline. It is extremely stable at ambient conditions, and often is the end product of the transformation of other iron oxides. Magnetite is also known as black iron oxide, magnetic iron ore, loadstone, ferrous

ferrite, or Hercules stone. It exhibits the strongest magnetism of any transition metal oxide (Cornell & Schwertmann, 2003; Majewski & Thierry, 2007). Maghemite occurs in soils as a weathering product of magnetite, or as a product of heating of other iron oxides. It is metastable with respect to hematite, and forms continuous solid solutions with magnetite (Majewski & Thierry, 2007).

### 2.2.2 Magnetic Behavior of Iron Oxides

The iron atom has a strong magnetic moment due to four unpaired electrons in its $3d$ orbitals. When crystals are formed from iron atoms, different magnetic states can arise as shown in Fig. 2. In the paramagnetic state, the individual atomic magnetic moments are randomly aligned with respect to each other, and the crystal has a zero net magnetic moment. If this crystal is subjected to an external magnetic field, some of these moments will align, and the crystal will attain a small net magnetic moment. In a ferromagnetic crystal, all the individual moments are aligned even without an external field. A ferrimagnetic crystal, on the other hand, has a net magnetic moment from two types of atoms with moments of different strengths that are arranged in an antiparallel fashion (see Fig. 2.7). If the antiparallel magnetic moments are of the same magnitude, then the crystal is antiferromagnetic and possesses no net magnetic moment.

In a bulk ferromagnetic material, the magnetization $M$ is the vector sum of all the magnetic moments of the atoms in the material per unit volume of the material. The magnitude of $M$ is generally less than its value when all atomic moments are perfectly aligned, because the bulk material consists of domains (Fig. 2.8) with each domain having its own magnetization vector arising from an alignment of atomic magnetic moments within the domain. The magnetization vectors of all the domains in the material may not be aligned, leading to a decrease in the overall magnetization (Fig. 2.8). When the length scale of the material becomes small, however, the number of domains decreases until there is a single domain when the characteristic size of the material is below some critical size $d_c$.

**Table 2.2** Physical and magnetic properties of iron oxides (Cornell & Schwertmann, 2003)

| Properties | Iron oxide | | |
|---|---|---|---|
| | Hematite | Magnetite | Maghemite |
| Molecular formula | $\alpha$-$Fe_2O_3$ | $Fe_3O_4$ | $\gamma$-$Fe_2O_3$ |
| Density ($g/cm^3$) | 5.26 | 5.18 | 4.87 |
| Melting point (°C) | 1350 | 1583-1597 | - |
| Hardness | 6.5 | 5.5 | 5 |
| Type of magnetism | Weakly ferromagnetic or antiferromagnetic | Ferromagnetic | Ferrimagnetic |
| Curie temperature (K) | 956 | 850 | 820-986 |
| MS at 300 K ($A-m^2/kg$) | 0.3 | 92-100 | 60-80 |
| Standard free energy of formation $\Delta G_f°$ (kJ/mol) | -742.7 | -1012.6 | -711.1 |
| Crystallographic system | Rhombohedral | hexagonal Cubic | Cubic or tetrahedral |

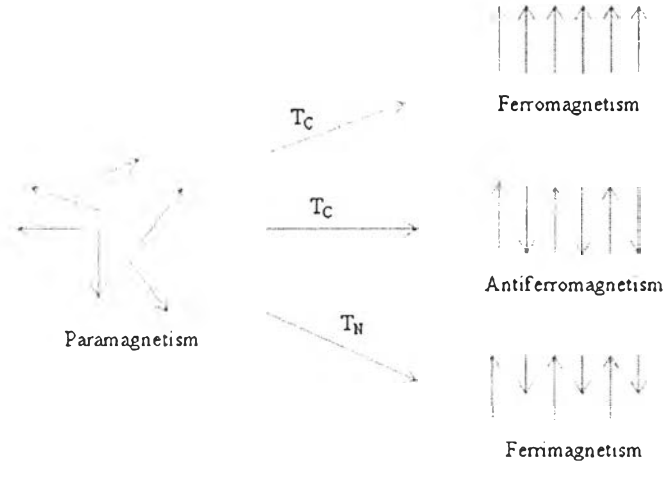


**Figure 2.7** Alignment of individual atomic magnetic moments in different types of materials.

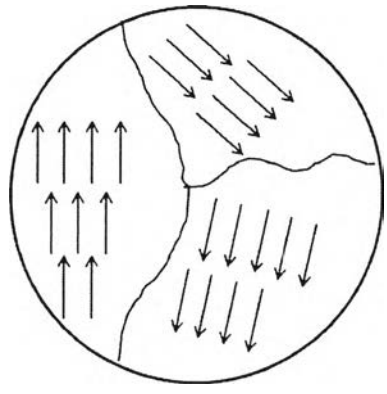

**Figure 2.8** Magnetic domains in a bulk material.

If an external magnetic field of strength $H$ is applied to a ferromagnet of magnetic strength $M$, the magnetization curve of Fig. 2.9 is obtained showing that M increases with $H$ until a saturation value $M_S$ is reached. The magnetization curve displays a hysteresis loop, because all domains do not return to their original orientations when $H$ is decreased after the saturation magnetization value is attained. Thus, when $H$ returns to zero, there is a remnant magnetization $M_R$ which can only be removed by applying a coercive field $H_C$ in the opposite direction to the initially applied field. A single domain magnetic material has no hysteresis loop and is said to be superparamagnetic. Iron oxide nanoparticles smaller than about 20 nm often display superparamagnetic behavior at room temperature (Cornell & Schwertmann, 2003).

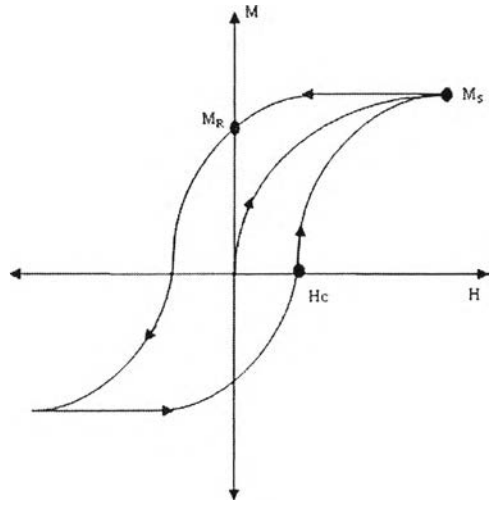


**Figure 2.9** Magnetization M as a function of an applied magnetic field H.

## 2.3 Silver Particle

### 2.3.1 Preparation of Silver Nanoparticle

The most common methods used for the preparation of colloidal suspensions of metals (silver including) are the reduction of corresponding metal cation. In addition to the inorganic or organic reduction agents, the ultrasound, the UV radiation and gamma radiation can be used to initiate the reduction.

#### *2.3.1.1 Laser Ablation*

Laser ablation of silver macroscopic material (e.g. silver foil) is a novel and promising physical method for the silver colloid particles preparation. The advantages of this method are namely an ease of the process, versatility with regard to metal identity or choice of solvent as well as the absence of additive chemical agent residues. Metal particles prepared by laser ablation are chemically pure.

#### *2.3.1.2 The Reduction by the Action of Ultrasound*

Except for the above-mentioned usage of ultrasound in a dispersion method of colloid particle preparation it can be also as a condensation method. The ultrasound is capable to decompose water into hydrogen and hydroxyl radicals. Subsequent reactions with suitable additives yield organic radicals which

act as reducing agents. By sonification of aqueous silver salts solutions in the presence of surfactants the silver particles were prepared.

*2.3.1.3 The Reduction by the Action of Gamma Radiation*

For the preparation of submicroscopic silver particles a direct radiolysis of silver salt aqueous solutions can be used. The advantage of this preparation method is that minimum interfering chemical substances are introduced into the reduction mixture, which could possibly absorb onto particles and thus change their specific properties. During the irradiation of silver salt solution under hydrogen gas atmosphere hydrated electrons and hydrogen atoms are formed, which reduce the silver ions to form silver nanoparticles.

*2.3.1.4 The Reduction by the Action of UV Radiation*

Photochemical method of colloid particle preparation using UV radiation yields the particles with properties similar to the particles produced by the above mentioned radiolytic method. Mercury discharge lamp is often used as the source of UV radiation. In addition to silver salt and evental stabilizers the reaction mixture contains suitable organic substance whose interaction with UV radiation generates radicals which reduce silver ions.

*2.3.1.5 The Reduction by Chemical Agents*

The most commonly used method for the preparation of silver sols is the reduction of silver salt by sodium borohydride ($NaBH_4$), which generated free electrons and reduce silver ions to form silver particle. By the standard methods of silver salt reduction by $NaH_4$ the particles with units of nanometers sizes and narrow size distribution are prepared.

2.3.2 Optical Properties of Silver Nanoparticle

Conduction electrons and ionic cores in metal form a plasma state. When external electric fields (electro-magnetic waves, electron beams etc.) are applied to a metal, electrons move so as to screen perturbed charge distribution, further move beyond the neutral states, and again return to the neutral states and so on. This collective motion of electrons is called a "Plasma Oscillation" as shown in Figure 2.10. The surface plasmon resonance is a collective excitation mode of the plasma localized near the surface. Electrons confined in a nanoparticle conform the

surface plasmon mode. The resonance frequency of the surface plasmon is different from an ordinary plasma frequency. The surface plasmon mode arises from the electron confinement in the nanoparticle. Since the dielectric function tends to become continuous at the interface (surface), the oscillation mode shifts from the ordinary plasma resonance and exponentially decays along the depth from the surface.

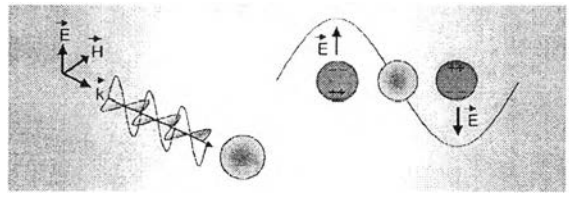


**Figure 2.10** Plasmon oscillation of the free electron on the surface of metal nanoparticle.

## 2.4 Zinc Oxide Particles

### 2.4.1 ZnO Nanoparticles and Nanorods

Recently, ZnO has been found highly attractive because of its remarkable application potential in solar cells, sensors, displays, gas sensors, varistors, piezoelectric devices, electro-acoustic transducers, photo-diodes and UV light emitting devices, sun-screens, gas sensors, UV absorbers, anti-reflection coatings, photo-catalysis and catalyst (Pan, Dai, & Wang, 2001; Arnold, Avouris, Pan, & Wang, 2003; Xiong, Gu, You, & Wu, 2003). Potentiality of ZnO for removing dye from textile effluent under UVC light has been proved by Behnajady, Modirshahla, & Hamzavi (2006).

ZnO is an n-type semi-conductor as well as $TiO_2$. Only these two metaloxides, among the 3d transition metal oxide semi-conductor series, have sufficient stability on photo-excitation state. The band gap energy of ZnO is 3.37 eV. Their stability can be justified with decreasing the possibility of electron–hole re-combination. This phenomenon is related to dissimilar parity of produced photo-

excited electron–hole pair under UV irradiation (Vigneshwaran, Kumar, Kathe, Varadarajan, & Prasad, 2006).

ZnO nano-particles have some advantages, compared to silver nano-particle, such as lower cost, white appearance (Vigneshwaran, Kumar, Kathe, Varadarajan, & Prasad, 2006) and UV-blocking property. ZnO powders can absorb infra-red light and infra-red electromagnetic wave with 5–16.68 dB in the range of 2.45–18 GHz (Vigneshwaran, Kumar, Kathe, Varadarajan, & Prasad, 2006). ZnO is also used to reinforce polymeric nano-composites (Vigneshwaran, Kumar, Kathe, Varadarajan, & Prasad, 2006). They also appeared for enhancement wear resistant phase and anti-sliding phase in composites as a consequence of their high elastic modulus and strength (Xu, & Xie, 2003). Li and colleagues have investigated the durability of anti-bacterial activity of nano ZnO functionalized cotton fabric to sweat. They have treated cotton fabrics at a concentration of 11 g/l ZnO and padded them to 100% wet pick-up. The durability of anti-bacterial activity of the finished fabric in alkaline, acidic and inorganic salt artificial sweat solution has been evaluated. Results showed better salt and alkaline resistances than acid resistances for the treated fabrics (Li, Chen, & Jiang, 2007). A negative surface charge has been deduced for ZnO nano-particles and illumination can increase anti-bacterial performance compared to normal conditions (Li, Chen, & Jiang, 2007).

Tetrapod-like nano-particle ZnO was also used for producing acrylic composite resin (Xu, & Xie, 2003). ZnO nano-belts, nanowires, nanotubes and nanocages have been also produced by Pan, Dai, & Wang (2001).

Xu & Cai (2008) have grown ZnO nano-rod on cotton fabric samples through the dip-pad-cure process. However, the control mechanism of nano-rod growth has not been described. They have tried to cover the prepared nano rod with a super hydrophobic agent to produce a cotton fabric with super hydrophobic properties based on the Cassie and Baxter theory (Eq. 1).

$$\text{Cos } \theta' = f_1 \text{ Cos } \theta_S - f_2 \text{ Cos } \theta_V \quad \text{---------- (Eq. 1)}$$

where $f_1$ is the fraction of fluid area in contact with the substance, and $f_2$ is the fraction of the fluid area in contact with air. $\theta'$ indicates the contact angle at a surface composed of solid and air. $\theta_S$ and $\theta_V$ are the corresponding water contact

angles on smooth solid surface and vapor surface. The equation can be used for hydrophobic surfaces that trap air in the hollows of the rough surface and the liquid–air contact angle ($\theta_V$) is 180° (Xu, & Cai, 2008; Genzer, & Efimenko, 2006).

2.4.2 Antibacterial Mechanism of Zinc Oxide Nanoparticles

The antibacterial properties were found in both microscale and nanoscale formulations (Jones, Ray, Ranjit, & Manna, 2008). Due to the high specific surface area of ZnO nanoparticles, the valence electron of nanoparticles could react with visible light. The theme of particle-induced reactive-oxygen-species (ROS) production and oxidative injury inside bacterial cells has become an established paradigm underlying the ZnO antibacterial mechanism, as shown in figure 2.11.

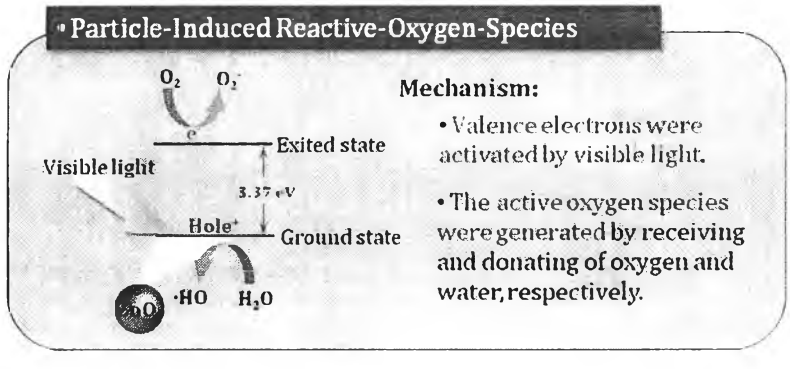


**Figure 2.11** Mechanism of particle-induced reactive-oxygen-species (ROS).